Atmos. Chem. Phys. Discuss., 14, 9903–9950, 2014
www.atmos-chem-phys-discuss.net/14/9903/2014/
doi:10.5194/acpd-14-9903-2014

Atmospheric Chemistry and Physics Discussions

Regional-scale simulations of fungal spore aerosols using an emission parameterization adapted to local measurements of fluorescent biological aerosol particles

M. Hummel[1], C. Hoose[1], M. Gallagher[2], D. A. Healy[3], J. A. Huffman[4], D. O'Connor[3], U. Pöschl[5], C. Pöhlker[5], N. H. Robinson[2], M. Schnaiter[1], J. R. Sodeau[3], E. Toprak[1], and H. Vogel[1]

[1]Institute for Meteorology and Climate Research, Karlsruhe Institute of Technology, Karlsruhe, Germany
[2]The Centre for Atmospheric Sciences, The University of Manchester, Manchester, UK
[3]Centre for Research into Atmospheric Chemistry, Department of Chemistry, University College Cork, Cork, Ireland
[4]Department of Chemistry & Biochemistry, University of Denver, Denver, Colorado, USA
[5]Biogeochemistry Department and Multiphase Chemistry Department, Max Planck Institute for Chemistry, Mainz, Germany

Received: 18 February 2014 – Accepted: 4 April 2014 – Published: 16 April 2014

Correspondence to: M. Hummel (matthias.hummel@kit.edu)

Published by Copernicus Publications on behalf of the European Geosciences Union.

ACPD
14, 9903–9950, 2014

Abstract

Fungal spores as a prominent type of primary biological aerosol particles (PBAP) have been incorporated into the COSMO-ART regional atmospheric model, using and comparing three different emission parameterizations. Two literature-based emission rates derived from fungal spore colony counts and chemical tracer measurements were used as a parameterization baseline for this study. A third, new emission parameterization was adapted to field measurements of fluorescent biological aerosol particles (FBAP) from four locations across Northern Europe. FBAP concentrations can be regarded as a lower estimate of total PBAP concentrations. Size distributions of FBAP often show a distinct mode at approx. 3 µm, corresponding to a diameter range characteristic for many fungal spores. Previous studies have suggested the majority of FBAP in several locations are dominated by fungal spores. Thus, we suggest that simulated fungal spore concentrations obtained from the emission parameterizations can be compared to the sum of total FBAP concentrations. A comparison reveals that parameterized estimates of fungal spore concentrations based on literature numbers underestimate measured FBAP concentrations. In agreement with measurement data, the model results show a diurnal cycle in simulated fungal spore concentrations, which may develop partially as a consequence of a varying boundary layer height between day and night. Measured FBAP and simulated fungal spore concentrations also correlate similarly with simulated temperature and humidity. These meteorological variables, together with leaf area index, were chosen to drive the new emission parameterization discussed here. Using the new emission parameterization on a model domain covering Western Europe, fungal spores in the lowest model layer comprise a fraction of 15 % of the total aerosol mass over land and reach average number concentrations of 26 L^{-1}. The results confirm that fungal spores and biological particles may account for a major fraction of supermicron aerosol particle number and mass concentration over vegetated continental regions and should thus be explicitly considered in air quality and climate studies.

ACPD
14, 9903–9950, 2014

1 Introduction

Particles emitted from biological sources are a miscellaneous and omnipresent group of the Earth's atmospheric aerosols (Elbert et al., 2007; Després et al., 2012). These primary biological aerosol particles (PBAP) can be transported over large distances and their impacts are studied by various fields of research, such as atmosphere science, agricultural research, biogeography and public health (Burrows et al., 2009). PBAP are solid airborne particles of biological origin and include microorganisms or reproductive units (e.g. bacteria, fungi, spores, pollen or viruses) as well as excretions and fragments of biological organisms (e.g. detritus, microbial fragments or leaf debris) (Després et al., 2012). Typical sizes range from <0.3 µm for viruses to diameters of single bacteria (0.25–3 µm), bacteria agglomerates (3–8 µm), fungal spores (1–30 µm), and up to 1–100 µm for airborne pollen (Jones and Harrison, 2004; Shaffer and Lighthart, 1997; Després et al., 2012).

The share of atmospheric aerosol composition belonging to PBAP is large and possibly underestimated (Jaenicke et al., 2007), but is also very uncertain. Estimates of relative PBAP fraction from global models and local measurements reveal large differences between reports. On one hand, the calculated global number concentration of PBAP (zonal annual mean surface concentrations of 10^{-2}–10^{-1} cm^{-3}) is below mineral dust (65 cm^{-3}) or soot (1000 cm^{-3}) concentrations by several orders of magnitude (Hoose et al., 2010b). Modeling studies yielded global source strengths of ∼ 10 Tg yr^{-1} (plant debris and fungal spores, Winiwarter et al., 2009), 56 Tg yr^{-1} (Penner, 1995), 78 Tg yr^{-1} (bacteria, fungal spores and pollen, Hoose et al., 2010a), 164 Tg yr^{-1} (Mahowald et al., 2008) and 312 Tg yr^{-1} (bacteria, fungal spores and pollen, Jacobson and Streets, 2009) for different PBAP components. On the other hand, measurements of continental boundary layer air in remote vegetated regions indicate that the mass fraction of PBAP in the coarse particle size range can be as high as ∼ 30 % (> 0.2 µm, Siberia, Matthias-Maser et al., 2000) or 65–85 % (> 1 µm, Amazonia, Martin et al., 2010; Pöschl et al., 2010; Huffman et al., 2012).

ACPD
14, 9903–9950, 2014

Like all other aerosol particles, PBAP can influence the Earth's climate by forcing the radiation budget directly (by absorbing or scattering radiation) and indirectly (by affecting cloud microphysics) (Forster et al., 2007). The direct PBAP effect on climate is difficult to estimate, because evaluations of the atmospheric PBAP concentration vary by several orders of magnitude when taking spatial and temporal divergences into account. Describing the radiative properties of PBAP is complicated, because their size ranges from fine to coarse (up to 100 µm in diameter) and in many cases their shapes are non-spherical and not accurately known. Hence, the applicability of Mie scattering theory is limited (Després et al., 2012). However, the direct PBAP effect on global and regional climate is generally assumed to be small due to low average concentrations, in contrast to the numbers of sub-micron absorbing and scattering aerosols. The indirect PBAP effect on climate is caused by PBAP that act as cloud condensation nuclei (CCN) and/or as ice nuclei (IN). Generally, changing aerosol populations by increasing nuclei concentrations or behavior can alter the microphysical properties of clouds, thus influencing the climate system (Forster et al., 2007). Most PBAP are assumed to be good CCN, because their surface area is large compared to most other aerosol species (Petters and Kreidenweis, 2007; Ariya et al., 2009) and thus may act as so-called giant CCN (Pöschl et al., 2010). Here, the Kelvin effect can be neglected when describing water vapor condensation, and thus activation and growth proceeds quickly (Pope, 2010). Some particles of biological origin (e.g. *P. syringae* bacteria and some fungal species) have been found to efficiently nucleate ice growth at relatively high temperatures (Després et al., 2012; Murray et al., 2012; Hoose and Möhler, 2012; Morris et al., 2004, 2013; Haga et al., 2013). Biological particles have been observed ubiquitously in precipitation, fog, and snowpack (e.g. Christner et al., 2008), in clouds from airborne measurements (e.g. DeLeon-Rodriguez et al., 2013) and have been shown to be important fractions of IN measured at ground level (e.g. Huffman et al., 2013; Prenni et al., 2009, 2013). These bio-IN may be important to ice nucleation in mixed-phase clouds at temperatures warmer than −15 °C (DeMott and Prenni, 2010), and therefore could influence atmospheric radiative properties on up to regional scales. In

ACPD
14, 9903–9950, 2014

regimes colder than that, mineral dust particles and other ice nucleators are also active and the relative atmospheric abundance of PBAP is probably too small to contribute significantly to formation and evolution of these colder clouds.

The methods for identifying and detecting PBAP are challenging and many different PBAP can introduce significant detection biases. Particle diameter often plays heavily into PBAP detection and characterization, and it should be noted that large discrepancies can exist between physical and aerodynamic diameter measurements (Huffman et al., 2010; Reponen et al., 2001). PBAP concentrations can be obtained either by online techniques, in which samples are analyzed by advanced instrumentation in real-time, or by offline measurement techniques. If measured offline, samples of airborne biological particles are stored under refrigeration and common methods include analysis by microscopy (stained or unmodified), by cultivation of the sample on growth media, and by amplification and detection of genetic material by sequencing or electrophoretic separation. Chemical and optical properties of PBAP samples or their tracers can be monitored in real time by: chromatography, mass spectrometry, fluorescence spectrophotometry, LIDAR, and flow cytometry. Short overviews of PBAP analysis techniques have been given by Caruana et al. (2011) and Després et al. (2012).

This paper focuses on the mesoscale simulation of atmospheric concentrations of fungal spores. The COSMO-ART limited-area model is used for the simulations and the setup includes a model domain covering most parts of Europe with a horizontal resolution of 14 km. Two different fungal spore emission parameterizations (Heald and Spracklen, 2009; Sesartic and Dallafior, 2011) are tested by comparing their number concentrations to online laser-induced fluorescence (LIF) measurements of airborne fluorescent biological particles. Additionally, a new emission parameterization adapted to these measurements is introduced. Field data used here comes from a real-time measurement technique that detects the intrinsic (i.e. unstained) fluorescence signal, after UV excitation, of fluorophores commonly present in most biological materials. Detected particles are categorized as fluorescent biological aerosol particles (FBAP),

ACPD
14, 9903–9950, 2014

which may broadly be considered a lower limit for the abundance of PBAP (Huffman et al., 2010; Pöhlker et al., 2012). FBAP were measured at four different locations (Table 1) concurrently during three focus periods in summer and fall 2010. The resulting FBAP size distribution is usually dominated by particles in the range from 2 µm to 4 µm, which is consistent with the size of fungal spores (Huffman et al., 2010, 2012, 2013; Pöschl et al., 2010, Healy et al., 2012a; Toprak and Schnaiter, 2013). Further, the concentration of FBAP in a given air-mass is generally considered to underestimate PBAP concentration due to biological particles that exhibit very low levels of fluorescent emission (Huffman et al., 2012). To some extent, non-biological aerosol components can also be part of the fluorescence signal for fine particles (~ 1 µm) (Huffman et al., 2010; Toprak and Schnaiter, 2013). These factors contribute uncertainty to the parameterizations discussed here, however the overall ability of LIF techniques to provide real-time FBAP measurements allows first approximation measurements that can be enlightening.

2 Methodology

2.1 Model description

The COSMO-ART atmospheric model system is based on the forecast model of the German weather service, combined with an online coupled module for simulating the spatial and temporal distribution of reactive gaseous and particulate components (Vogel et al., 2009). Additionally, fungal spores are incorporated as an independent, monodisperse particle class (d_p = 3 µm).

Parameterizations for emission, sedimentation, and washout, which were originally developed for pollen dispersal, are included for this particle class (Helbig et al., 2004). Fungal spores are treated independently, as no interactions with other aerosols or gases (coagulation or condensation) are considered. The temporal development of

ACPD
14, 9903–9950, 2014

the fungal spore number concentration is calculated by:

$$\rho \frac{\mathrm{d}\Psi}{\mathrm{d}t} = -\nabla \cdot \boldsymbol{F}_\mathrm{T} - \frac{\partial}{\partial z} F_\mathrm{S} - \lambda \Psi - \frac{1}{N} \frac{\partial}{\partial z} F_\mathrm{E} \tag{1}$$

with the number mixing ratio of fungal spores being

$$\Psi = \frac{N_\mathrm{f}}{N}, \tag{2}$$

and the number concentration of fungal spores N_f, the total number of particles and air molecules N per m^3, the air density ρ, the turbulent flux $\boldsymbol{F}_\mathrm{T}$, the sedimentation flux F_S, a washout coefficient λ and a vertical emission flux F_E (Vogel et al., 2008). The turbulent flux is calculated by $\boldsymbol{F}_\mathrm{T} = \overline{\rho v' \Psi'}$, incorporating the turbulent fluctuations of wind speed v' and fungal spore number mixing ratio Ψ'. Fungal spore sedimentation is calculated by $F_\mathrm{S} = \rho \Psi v_\mathrm{s}$. The fungal spore settling velocity v_s is calculated by applying the volume-equivalent particle diameter $d_\mathrm{e} = 2\sqrt[3]{a^2 b}$, with $a = 2\,\mu\mathrm{m}$ and $b = 5\,\mu\mathrm{m}$ (Yamamoto et al., 2012) being the major and minor radius of a prolate spheroid. This results in:

$$v_\mathrm{s}^2 = \frac{4 \rho_\mathrm{p} d_\mathrm{e} g}{3 \rho c_\mathrm{d}} \tag{3}$$

where $\rho_\mathrm{p} = 1\,\mathrm{g\,cm}^{-3}$ is the spore density (Trail et al., 2005; Gregory, 1961) and c_d the drag coefficient (Aylor, 2002). The calculation of the washout coefficient is based on the assumption of raindrops being much larger than aerosol particles and having a much higher terminal fall velocity. It yields:

$$\lambda(d_\mathrm{p}) = \int_0^\infty \frac{\pi}{4} D_\mathrm{D}^2 v_\mathrm{t}(D_\mathrm{D}) E(d_\mathrm{p}, D_\mathrm{D}) n(D_\mathrm{D}) \mathrm{d}D_\mathrm{D} \tag{4}$$

ACPD
14, 9903–9950, 2014

(Rinke, 2008). d_p and D_D are the diameters of particles and raindrops, respectively, $v_t(D_D)$ is the terminal fall velocity, E is a collision efficiency and $n(D_D)$ is the size distribution of the raindrop number concentration. For fungal spores with a spherical diameter of 3 µm, the collision efficiency E with 0.1 mm and 1 mm droplets is approximately 0.085 and 0.3, respectively.

Adapting the model for simulations of fungal spores requires inclusion of an emission flux F_E in the source term of Eq. (1) by means of an emission parameterization which will be described in the next section.

Together with fungal spore simulations COSMO-ART is used to compute the mass concentration of major atmospheric aerosol components. Hence, the proportion of fungal spores with respect to the dry aerosol mass can be estimated (Sect. 3.3). In addition to primary aerosol emissions, further gaseous emissions given by the EMPA emission dataset (Sect. 2.3) are taken into account. Partitioning of inorganic aerosol components between the gases at particulate phase is simulated by the ISORROPIA II module (Fountoukis and Nenes, 2007). Condensation on fungal spore aerosols is not included. The contribution of secondary organic aerosols (SOA) to the particles is handled by condensation of oxidized volatile organic compounds as described by Schell et al. (2001). When soot aerosols are not involved as a solid nuclei enabling condensation, clusters build by gas-to-particle conversion via binary nucleation of sulfuric acid and water. They are computed as an individual particle mode. All aerosol particles including these chemical compounds are assumed to be internally mixed. A soot mode without mixing of other chemical compounds is included as particles that are emitted directly into the atmosphere. Anthropogenic primary aerosols (aPA) in the coarse size range (< 10 µm) are treated as a separate mode. Detailed descriptions are given in Vogel et al. (2009). Furthermore, sea salt is included in the model simulation and its emission is related to sea water temperature and wind speed (Lundgren et al., 2013). No desert dust emissions are included, as the model domain does not cover the corresponding emission regions and no transport into the model domain is taken into account.

ACPD
14, 9903–9950, 2014

2.2 Emission parameterization of fungal spores

In literature, a constant emission rate was used as input of a global chemical transport model to represent the magnitude and range of measured concentrations of mannitol as a molecular tracer for basidiospores (Elbert et al., 2007; Heald and Spracklen, 2009). Broad geographical differences can be included in the emission flux by distinguishing between ecosystems. While reviewing the measured data available on measured fungal spore concentrations, Sesartic and Dallafior (2011) calculated number fluxes of fungal spore emissions for six different ecosystems (defined by Olson et al., 2001). Four of these emission fluxes were included into COSMO-ART, and coupled to ecosystem definitions by the GLC2000 (Global Landcover 2000 Database) (forest and shrubs) and Ramankutty et al. (2008) (grassland and crops). The sum of these fluxes, as defined by Sesartic and Dallafior (2011), are emitted from the land area fraction E_i of each ecosystem i ($\sum_i^n E_i = 1$ for n number of ecosystems), gives the total emission flux $F_E = F_{S\&D}$ in $m^{-2}\,s^{-1}$ of Eq. (1) for fungal spores:

$$F_{S\&D} = 214\,m^{-2}\,s^{-1}E_{forest} + 1203\,m^{-2}\,s^{-1}E_{shrub} + 165\,m^{-2}\,s^{-1}E_{grassland} + 2509\,m^{-2}\,s^{-1}E_{crop} \quad (5)$$

Additionally, a second emission parameterization was tested, which varies as a function of meteorological and surface conditions. Jones and Harrison (2004) reviewed the relations determined when analyzing the observed fungal spore concentrations and atmospheric factors. Seasonal variations can be explained by changes in the leaf area index (LAI). This was verified by correlation to the observed mannitol concentrations. Among the drivers of day-to-day variations, specific humidity (q_v) correlates best with the mannitol concentrations (Heald and Spracklen, 2009). It was argued that though other atmospheric factors (e.g. temperature) may actually drive the correlation, this does not change correlation results and thus parameterizations can proceed without having information about the root drivers of fungal spore release. A constant emission rate was used here by linearly scaling LAI and q_v in order to give global

ACPD
14, 9903–9950, 2014

fungal spore concentrations matching the mean mannitol concentrations (Heald and Spracklen, 2009). In order to fit to the emission flux specified in Hoose et al. (2010a) for a spore diameter of 5 µm, a constant c is set to $c = 2315\,\mathrm{m^{-2}\,s^{-1}}$ to be appropriate for fungal spores with 3 µm in diameter. Based on the emission flux in Eq. (1), this gives an alternative source $F_E = F_{H\&S}$ of fungal spores in $\mathrm{m^{-2}\,s^{-1}}$:

$$F_{H\&S} = c\frac{\mathrm{LAI}}{\mathrm{LAI}_{max}}\frac{q_v}{q_{v,\,max}} \tag{6}$$

LAI is the leaf area index, q_v is the specific humidity at the surface, and their scaling factors adapted from tropical rain forest conditions are assumed to be $\mathrm{LAI}_{max} = 5\,\mathrm{m^2\,m^{-2}}$ and $q_{v,\,max} = 1.5\times10^{-2}\,\mathrm{kg\,kg^{-1}}$. In the COSMO-ART simulations LAI is horizontally distributed according to GLC2000 containing monthly variation and q_v is provided by the model as a meteorological variable.

2.3 Model domain and input data

The COSMO-ART mesoscale model system is driven by initial and boundary data for meteorological and aerosol and chemistry conditions. The meteorological conditions are updated every six hours and result from interpolation of the coarse grid operational atmospheric model analysis of the ECMWF (European Centre for Medium-Range Weather Forecasts). No initial and boundary concentrations are predefined for aerosols or gases. Therefore, all gaseous species are set to a climatological, homogeneously distributed initial concentration. The emission rates for chemical compounds included in the ART part are updated hourly. They are provided by EMPA (Swiss Federal Laboratories for Materials Science and Technology) based on the TNO/MACC (Monitoring Atmospheric Composition and Climate) inventory (Kuenen et al., 2011). The treatment of emissions for COSMO-ART can be found in Knote et al. (2011). Homogeneously distributed mass densities for each aerosol are used as initial conditions, together with the aerosol size distribution and particle density. Primary particle emissions are included

ACPD
14, 9903–9950, 2014

as parameterizations based on meteorological and surface conditions. Land use data and constant surface properties are derived from the GLC2000 database (Bartholomé and Belward, 2005). All parameters are post-processed to the rotated spherical coordinate system of COSMO-ART (Doms and Schättler, 2002). For the purpose of this paper, the model domain covers most parts of Western Europe from mainland Portugal to northern Finland, the longitudinal extension being 2849 km the latitudinal extension being 3803 km with a horizontal spacing of 0.125° ($\widehat{=}$ 14 km) on a rotated grid. In vertical direction the model reaches up to an altitude of about 24 km distributed over 40 terrain-following levels. The time stepping of the Runge–Kutta dynamical core is set to 30 s.

2.4 Auto-fluorescence measurements

Ambient aerosols can be roughly classified as biological or not by interrogating particles at characteristic wavelengths of excitation and measuring the resultant emission in a process called ultraviolet light-induced fluorescence (UV-LIF) (e.g. Hairston et al., 1997; Pan et al., 1999). In particular, the region of fluorescent excitation near 360 nm is often used as characteristic of certain cell metabolites present in all living cells, including riboflavin and reduced pyridine nucleotides (e.g. NAD(P)H). The region of excitation near 270 nm includes certain amino acids (e.g. tryptophan) contained in all proteins. However, many other biological fluorophores exist and the relationship between the measured fluorescence of complex biological particles and fluorophore assignment is very complex (Pöhlker et al., 2012, 2013).

Two instrument types were utilized at four locations for the comparison discussed in this paper. The ultraviolet aerodynamic particle sizer (UV-APS; TSI, Inc., Shoreview, MN, USA) measures particle size aerodynamically, excites individual particles using a single Nd:YAG laser pulse at 355 nm, and detects integrated fluorescent emission (non-dispersed) in a single wavelength region between 420 and 575 nm (Hairston et al., 1997; Brosseau et al., 2000; Huffman et al., 2010). The Waveband Integrated Bioaerosol Sensor (WIBS, versions 3 and 4; University of Hertfordshire, UK) measures

ACPD
14, 9903–9950, 2014

particle size optically and excites individual particles via two sequential pulses from a Xe-flash lamp, at 280 and 370 nm, respectively (e.g. Kaye et al., 2005; Foot et al., 2008). Fluorescence for each particle is then measured in one of two wavelength regions, resulting in three measured fluorescence parameters for each WIBS instrument named FL1_280, FL2_280, and FL3_370. See Gabey et al. (2010) and Robinson et al. (2013) for more details, including slight differences in WIBS-3 and WIBS-4 models. The number concentration of FBAP can be written as $N_{F,c}$ with subscripts referring to fluorescent and coarse particle size. The differences in the pairs of wavelengths used for fluorescence, as well as the possible differences in sensitivity between instruments, suggest that the term "FBAP" as determined by each instrument is not rigorously interchangeable, and it is critical to understand the method of analysis when comparing datasets. For example, the ambient FBAP number concentration as determined by UV-APS has been shown to be qualitatively consistent with the number concentration of particles that fluorescence in the WIBS FL3_370 channel, while the $N_{F,c}$ comparison between UV-APS and WIBS FL1_280 channel is relatively poor (Healy et al., 2014). Here we use the term FBAP from WIBS data to mean particles that exhibit fluorescence simultaneously in both channels FL1_280 and FL3_370.

Particle size can aide differentiation between biological particles classes observed, however the selectivity based on size alone is very uncertain. For example, and to a rough first approximation, it may be true that many FBAP $\sim$ 1 µm are single bacterial particles and that many FBAP 2–6 µm may be fungal spores or bacterial agglomerates (Shaffer and Lighthart, 1997). However, biological species can vary widely, and other FBAP classes (e.g. fragments of larger PBAP, internal components of burst pollen, the presence of other biological species) confound the simple assignment of FBAP based on size (Després et al., 2012).

Further, at least a fraction of fluorescent, supermicron particles are likely to come from non-biological sources, and thus could be counted as FBAP. These non-biological process include anthropogenic sources (e.g. polycyclic aromatic hydrocarbon particles from combustion and cigarette smoke), present most often in submicron particles

ACPD
14, 9903–9950, 2014

(Huffman et al., 2010), select oxidized organic aerosol particles (e.g. absorbing brown carbon particles) (Bones et al., 2010; Lee et al., 2013), and some humic-like substances (Gabey et al., 2013). For example, at the rural, elevated site of Puy de Dôme, France, WIBS-3 FBAP measurements were compared to results from fluorescence microscopy paired with staining of fungal spores and bacteria. These results suggest that the real-time UV-LIF measurements indeed track the diurnal cycle of the bacteria concentration, but that non-biological particles still contributed significantly to fluorescent particle number (Gabey et al., 2013).

Virtually every ambient measurement study performed with the WIBS or UV-APS to date has shown a dominant FBAP mode peaking at 2–4 µm in size (Huffman et al., 2010, 2012, 2013; Gabey et al., 2010; Toprak and Schnaiter, 2013). For example, the FBAP size distributions measured at each of the four sampling locations discussed here is shown in Fig. 1, highlighting the common presence of the 2–4 µm peak. It has been proposed that fungal spores and bacteria agglomerates are the most dominant biological aerosols in this size range (Jones and Harrison, 2004; Després et al., 2012; Fang et al., 2008) and that the FBAP signal in this size range is typically dominated by fungal spores. This was corroborated in more detail for a remote Amazonian site using FBAP analysis along with fluorescence microscopy of stained filter samples (Huffman et al., 2012), but has not yet been rigorously tested in other environments. Other microscopy and DNA-based studies have suggested that fungal spores constitute the largest fraction of PBAP in the 2–4 µm size (e.g. Graham et al., 2003; Lin and Li, 1996; Burch and Levetin, 2002). Bauer et al. (2008) showed that fungal spores account for an average of 60 % of the organic content in the particulate matter in a size range of 2–10 µm in rural and urban areas of Vienna, Austria.

ACPD
14, 9903–9950, 2014

3 Results

3.1 Comparison of time series of measured FBAP and simulated fungal spores

Fungal spore concentrations simulated using the emission flux given in Eqs. (5) and.(6) according to Heald and Spracklen (2009) and Sesartic and Dallafior (2011) were first compared to FBAP measurements without further adjustment. An overview of time series for all measurements and simulations discussed here is shown in Fig. 2 by a box-and-whiskers plot. Time periods for each of three case studies (Table 1) were chosen as exemplary periods when UV-LIF instruments were operating simultaneously at a minimum of two locations, with no requirements applied with respect to environmental conditions. For the statistical analysis, FBAP measurements were averaged over one hour periods in order to be consistent to the model output time steps. For most time periods at Karlsruhe and Hyytiälä the simulated fungal spore concentrations are smaller than the measured FBAP concentrations (Fig. 2). This difference is highest at Hyytiälä in August 2010. At Hyytiälä in July and at Manchester and Killarney in August, the Heald and Spracklen (2009) emission ($F_{H\&S}$) gives median concentration values which agree reasonably well with the measurements. During October, the fungal spores number concentrations based on constant emission fluxes given by Sesartic and Dallafior (2011) ($F_{S\&D}$) agree best with the measured FBAP concentrations. Long-term analysis of FBAP measurements, including periods at the Karlsruhe (Toprak and Schnaiter, 2013) and Hyytiälä site (Schumacher et al., 2013) discussed here, shows an annual cycle of average FBAP number concentrations peaking in summer and lowest in winter. Thus, a simulation based on a constant emission flux may not be appropriate to reproduce the FBAP concentrations.

Figures 3 to 6 show a series of one-week long case studies, each representing two measurement sites. The plots show comparisons between simulation and measurement time series for each station. The simulated fungal spore number concentration is given for the model grid point closest to the measuring site. Due to model spin-up, the first six hours of the simulated fungal spore concentrations are removed from the

ACPD
14, 9903–9950, 2014

figures and are not included in the analysis. The total precipitation calculated by the model is shown by gray bars with the ordinate on the right hand side of the figure. The simulated boundary layer height is also included at the bottom of each panel in the figures.

Measured FBAP number concentrations often exhibit distinct diel (24 h) cycles with a maximum in the morning hours or around midnight and a minimum around noon. These features have been consistently reported by most studies discussing temporal behavior of FBAP (Gabey et al., 2010; Huffman et al., 2010, 2012; Toprak and Schnaiter, 2013). Here, a similar diel cycle is frequently obtained from simulations, and the simulated fungal spore concentrations often anti-correlate with the simulated boundary layer height (h_{PBL}) (Figs. 3 to 6). The measured FBAP concentrations often qualitatively track the general pattern of simulated h_{PBL}, however the magnitude of concentration change and the timing is often not consistent. For example, on 24 and 25 July at the Karlsruhe site (Fig. 3a) a boundary layer compression during the night leads to an increase in the simulated fungal spore concentrations by a factor of ~ 4, and during day the concentrations decreases as the boundary layer rises again. In this case, the measured FBAP concentrations are in relatively good agreement with the simulated fungal spore numbers, with $N_{F,c}$ dropping slowly during the day on 24 and 27 July, and to a rate closer to the simulations on 25 July. This suggests that FBAP concentrations were likely influenced, at least partially, by the changing boundary layer height, though diel changes in biological emission are also likely to influence diel FBAP patterns. A similar temporal pattern in simulated fungal spore concentrations is shown in Fig. 4a, where a maximum in h_{PBL} at 12 and 13 October occurs approximately coincident with a minimum in the simulated number concentration. In this case, however, the measured FBAP concentrations do not reflect the diel pattern of the simulations. On 31 August (Fig. 5a), measured FBAP and simulated fungal spore number concentration increase simultaneously and parallel to the boundary layer compression, but the increase is more intense for FBAP measurements than for spore simulations. Additionally, at Manchester between 31 August and 1 September (Fig. 6a) measured and

ACPD
14, 9903–9950, 2014

simulated concentrations are in good agreement. Distinct minima and maxima clearly anti-correlate with the minima and maxima of the boundary layer height. In contrast, during the same time period in Killarney (Fig. 6b), small changes in the boundary layer were simulated along with minor changes in fungal spore concentrations. In this case, measured FBAP concentrations qualitatively reflect the same temporal pattern of number concentration, but show poor trend consistency with h_{PBL}. The magnitude of diel FBAP concentration change was similar throughout the week shown, whereas h_{PBL} showed large diel variations between 26 and 30 August and relatively no change in h_{PBL} from 30 August to 1 September. Figures 3b, 4b, and 5b also show diel FBAP concentration changes that correlate poorly with simulated h_{PBL}. We conclude that (i) simulated fungal spore concentrations are sensitive to changes in the simulated boundary layer height, by extension, that (ii) diel cycles of FBAP concentrations are likely to be partially influenced by diel cycles of boundary layer height, but that (iii) the development of the FBAP concentration is in addition influenced by daily cycles in biological emission processes, including those of fungal spores and other PBAP classes. These competing effects are impossible to separate by this analysis.

A comparison of measured FBAP and simulated fungal spore number concentrations for July 2010 is shown in Fig. 3. At the measurement site of Karlsruhe, diel cycles were found in the simulated and measured time series, with constantly lower concentrations being obtained from simulations based on emission parameterizations given in literature. When precipitation occurs in the simulation, the simulated fungal spore concentrations decrease due to washout and the diel development of the concentration is interrupted. Afterwards, the simulated concentrations quickly return to the previous baseline. At Hyytiälä a strong decrease in simulated fungal spore concentration on 24 July precisely overlaps with the simulation of precipitation. After hitting a minimum value during simulated precipitation, the simulated fungal spore concentration increases steadily for two days as a result of a post-frontal shift in wind direction and decrease in wind speed. The increase is also reflected in the measured FBAP concentrations. However, the simulated precipitation values do not always coincide with

ACPD
14, 9903–9950, 2014

precipitation at the site, as was the case in this instance. As a result of no rain falling at the site on 24 July, the measured FBAP concentration was not affected by the simulated rain. While this example shows that uncertainty in local meteorology contributes uncertainty to the aerosol output of the model, washout from precipitation remains an important modeled process for estimating FBAP concentrations. Additionally, other dynamic processes are known to affect FBAP concentrations. For example, FBAP has been shown to increase dramatically during rainfall, a process reported recently for both a site in Colorado (Huffman et al., 2013) and also at the Hyytiälä site (Schumacher et al., 2013). The reasons for this FBAP increase are unclear, but are thought to be related to mechanical ejection from terrestrial surfaces as a result of rain droplet splash (Huffman et al., 2013). These effects are known to be dependent on the local geography and ecology, however, and are outside the scope of the presented emission parameterizations.

During the simulation period of October 2010, the simulated fungal spore number concentrations $F_{H\&S}$ are consistently below the measured FBAP concentrations at the sites of Karlsruhe and Hyytiälä, whereas $F_{S\&D}$ matches the relative magnitude of the measurements more closely in both cases (Fig. 4). At Karlsruhe, concentrations simulated by each emission parameterization follow a distinct diel cycle and increase slightly through the week, reaching concentration maxima on 15 October. The measured FBAP concentration develops differently, with only very weak diel cycle present from 11 to 14 October, and showing little relationship to the simulated h_{PBL}, as discussed above.

At the end of August 2010, four different measurement series were available for a comparison to fungal spore simulations (Figs. 5 and 6). The measured time series of FBAP number concentrations generally exhibit diel cycles, as discussed. The absolute FBAP concentration at Hyytiälä was consistently highest, when comparing all four sites. This trend is even more obvious when comparing the median concentrations on a linear scale (Fig. 2). As a result, concentrations simulated from the literature-based parameterizations under-predict measurements by the greatest margin at Hyytiälä. This under-prediction is likely a result of the persistent precipitation simulated by the model

ACPD
14, 9903–9950, 2014

and is an indication that precipitation has a stronger influence on the simulated concentrations than changes in the boundary layer height. Measured rainfall during this period at Hyytiälä was less consistent than the model predicts, but occurred with episodic peaks. In all other August case studies, simulated fungal spore concentrations show relatively good agreement with FBAP measurements.

3.2 Development of a fungal spore emission parameterization by adaptation to FBAP measurements

Direct comparison between simulated fungal spores and measured FBAP reveals that in general the simulated concentrations systematically underestimate the measured concentrations (Fig. 7a). This difference is most distinct at Hyytiälä during the August case study and at Karlsruhe in the July and October case study. Here we suggest an improved parameterization, including meteorological and surface parameters identified earlier as drivers of fungal spore emissions. Additionally, new parameters driving fungal spore emissions have been investigated. The emission flux depends on these parameters and their fitting coefficients obtained from a regression analysis of the FBAP measurements. The new parameterization for fungal spore emissions has been incorporated into COSMO-ART and the resulting concentrations are included in Figs. 3 to 6.

The emission flux from the regression analysis is adjusted to an emission flux $F_{\mathrm{F,c}}$ estimated from the FBAP number concentration. For this, it is assumed that particles are evenly distributed throughout the planetary boundary layer and that the simulated fungal spore concentration negatively correlates with h_{PBL}. Together with a steady-state condition and neglecting horizontal exchanges with the surrounding air, the balance holds between the number concentration (N_{f}) and the emission rate ($F_{\mathrm{F,c}}$) together with the atmospheric lifetime of fungal spores (τ):

$$N_{\mathrm{f}} = \frac{F_{\mathrm{F,c}}\tau}{h_{\mathrm{PBL}}} \tag{7}$$

ACPD
14, 9903–9950, 2014

(Seinfeld and Pandis, 2006). The boundary layer height at the measurement site needs to be taken from the model simulation as it is not measured consistently. The fungal spore lifetime is assumed to be constant and is estimated with an initial value of one day, as given in literature for aerosol particles with 3 µm in diameter (Jaenicke, 1978). A new simulation of the fungal spore concentrations with the initial value of atmospheric spore lifetime reveals an underestimation compared to the FBAP measurements. As a remedy, the fungal spore lifetime is corrected to $\tau = 4\ 3/4$ h. The deviation from a lifetime of 3 µm particles given in literature may be attributed to the assumption of a constant vertical distribution of fungal spores with increasing altitude until boundary layer height. However, a ratio of approximately 1.75 between surface-level concentrations and mean concentrations within the boundary layer is too small to explain the discrepancy in lifetime.

Two types of instruments operating with different numbers of channels and detecting fluorescence at different wavelengths are used here for deriving an emission parameterization appropriate for fungal spores. The technical difference may lead to slightly deviating FBAP concentrations (Healy et al., 2014), because the WIBS instrument only counts particles as FBAP when a signal exceeds a threshold in both channels (Pöhlker et al., 2012; Gabey et al., 2010). Some fungal spores most abundant in the Earth's atmosphere and very common for fungal spores of 2–4 µm (*Cladosporium* sp., *Aspergillus versicolor, Penicillium solitum*) (Fröhlich-Nowoisky et al., 2012; Hameed and Khodr, 2001) only show a weak signal in the emission wavelength of 310 nm to 400 nm (Saari et al., 2013; Healy et al., 2014). This difference needs to be taken into account when comparing absolute concentrations of fungal spores and FBAP. During the time periods shown here, the WIBS indicate slightly lower FBAP concentrations than the UV-APS when comparing to the model results. In general, this feature is not always valid and detailed side-by-side comparisons between the two types of instruments are required to determine their behavior in terms of FBAP detection and estimation of the PBAP concentration. In the attempt to factor out the technical difference between the instruments, we assume that FBAP concentration can be multiplied by a constant factor

ACPD
14, 9903–9950, 2014

for the concentration values to match each other. The amount of FBAP given by the UV-APS may be represented best by WIBS channel FL3_370 (Sect. 2.4). The FBAP concentration given by the UV-APS is therefore reduced by a factor derived from the WIBS instrument as the mean ratio between channel FL3_370 and the total FBAP concentration $N_{F,c}$ (channels FL1_280 and FL3_370). The factor is estimated to be 2.2 and identical for WIBS data at Karlsruhe and Manchester. The difference is not taken into account in the comparison of the time series in Sect. 3.1, but corrected before applying Eq. (7).

Analyzing the meteorological and surface parameters of the model output, it was found that a better correlation with the measured FBAP concentrations is achieved for specific humidity rather than relative humidity, as it was reported for previous field measurements (Gabey et al., 2010; Toprak and Schnaiter, 2013; Di Filippo et al., 2013). During the time period in July 2010, the measured FBAP concentrations vary in a narrow range of specific humidity, which is not reproduced by the literature-based simulation. For this reason, the July case study was removed from the regression analysis. A dependence on the LAI is required in order to take the seasonal change into account and to distinguish among various regions. A combination of LAI and specific humidity in the regression has the advantage of reducing the fitting parameters. The same relation was chosen by Heald and Spracklen (2009) for the previously discussed emission parameterization. Additionally, surface temperature dependence as suggested by Di Filippo et al. (2013) is indicated by the time series and factored in a regression analysis. The parameters ($b_1 = 20.426$ and $b_2 = 3.93 \times 10^4$) are estimated to be the smallest sum of all squared residuals and result in a multiple linear regression giving an emission flux $F_E = F_{FBAP}$ in $m^{-2}\,s^{-1}$ for fungal spores fitted to FBAP measurements:

$$F_{FBAP} = b_1(T - 275.82\,K) + b_2 q_v LAI \quad (8)$$

where T is the surface temperature in K, q_v the specific humidity in $kg\,kg^{-1}$, and LAI the leaf area index in $m^2\,m^{-2}$. The parameter inside the parentheses is related to an

ACPD
14, 9903–9950, 2014

emission offset of the regression and covers unknown influences. The coefficient b_2 is approximately the same as the constants in the Heald and Spracklen (2009) emission for a particle diameter of 3 µm given in Eq. (6). The additional temperature dependence in Eq. (8) increases the fungal spore emission for temperatures above 275.8 K and lowers the emission for temperatures below this value.

The multiple linear regression yields a coefficient of determination of $R^2 = 0.4$. By comparing the simulated concentrations (based on F_{FBAP}) to the measured FBAP concentrations, it is found that they distribute more evenly along the 1 : 1 line (Fig. 7b). The statistical overview (Fig. 2) shows a better agreement between the median concentrations of simulation and measurement for the new emission parameterization than for the literature-based emissions, which is most obvious at Karlsruhe in August and at Hyytiälä in July. The new emission parameterization only slightly reduces the underestimations found for Hyytiälä during August.

Figure 8 shows the emission flux for late August 2010, following the new parameterization, horizontally distributed over a model domain covering Europe. Here, averaged over land areas of the domain, F_{FBAP} gives $1.03 \times 10^3\,\mathrm{m^{-2}\,s^{-1}}$. During July and October, the average flux is shifted to $1.4 \times 10^3\,\mathrm{m^{-2}\,s^{-1}}$ and $0.4 \times 10^3\,\mathrm{m^{-2}\,s^{-1}}$, respectively, mainly as a result of seasonal changes of LAI and T.

When analyzing the temporal development of the simulated fungal spore concentrations for each time series, F_{FBAP} mostly results in a slightly higher number concentration than $F_{\mathrm{H\&S}}$ or $F_{\mathrm{S\&D}}$ (Figs. 3 to 6). This is not the case for October 2010, where the F_{FBAP}-concentrations are in the range of the literature-based concentrations. A sharp decrease on 15 October at Hyytiälä, which is not reflected by the literature-based simulation, is caused by a rapid temperature change. Comparison for the August case study show that simulated F_{FBAP}-concentrations agree well with measured FBAP concentrations without overestimating the measurement at Manchester and Killarney, where literature-based simulations and measurements already correspond to each other. Only a slight overestimation can be found at Manchester, which might be

ACPD
14, 9903–9950, 2014

due to an urban measuring site that is not represented accurately by the model setup with its broad resolution.

3.3 Contribution of fungal spore to near-surface aerosol composition

For a comparison of simulated fungal spores to the dry aerosol chemical composition, the fungal spore mass concentration is calculated from the number concentration assuming monodisperse and spherical particles ($\rho_p = 1\,g\,cm^{-3}$; Sect. 2.1). The horizontally distributed near-surface (approximately 10 m above ground) fungal spore number concentration using F_{FBAP} is shown in Fig. 9. Concentrations simulated at the measurement locations are considerably lower than the high surface concentrations in the southern part of the model domain.

The simulated mass concentrations of each chemical aerosol compound are averaged over the land areas of the model domain and the time period of late August 2010 (Fig. 10). The total aerosol mass concentration is approximately $2.5\,\mu g\,m^{-3}$. Fungal spores distribute in the domain with an average number concentration of $26\,L^{-1}$ over land. This corresponds to an average mass concentration of fungal spores of $0.37\,\mu g\,m^{-3}$ which accounts for 15.4 % of the total simulated aerosol mass. The total aerosol mass excludes mineral dust as one of the main contributors to the chemical aerosol composition, which might lower the fraction of fungal spore mass considerably. A list of mass concentrations of the simulated chemical aerosol compounds, including fungal spores occurring at the measurement site, is given in Table 2. The fraction of fungal spores simulated for these sites varies between 9 and 2 %. FBAP mass concentrations calculated from the measured FBAP number concentrations are also listed in Table 2. Here, the same spherical particle diameter and particle density as for the fungal spore simulation is assumed. The FBAP number concentrations are averaged over the same time period as covered by the aerosol simulation. Their share of the aerosol mass ranges from 5 % at Manchester up to 64 % at Hyytiälä. For Karlsruhe and Killarney, the fractions calculated from the measurements are in good agreement with the fractions resulting from the simulated fungal spore mass concentrations.

ACPD
14, 9903–9950, 2014

4 Discussion and conclusions

FBAP measurements from four locations in Northern Europe were compared with simulated fungal spore concentrations. Fluorescent particles in the diameter range of 2–4 µm are highest in number concentration of FBAP measurements at the rural site near Karlsruhe, Germany (Huffman et al., 2010, 2012, 2013; Pöschl et al., 2010; Healy et al., 2012a; Toprak and Schnaiter, 2013). The diameter range for peak FBAP concentration matches closely with the modal size of many species of fungal spores known to be present in airborne concentrations. Simulated fungal spores have been adjusted to match this diameter. Contrary to that, an increase in number concentration towards small particles has been reported for some FBAP measurement series, but only a small fraction of particles could be counted as bacteria cells (Gabey et al., 2011; Huffman et al., 2010).

Comparison of simulations and measurements at four locations and the correlation of FBAP concentrations to meteorological and surface conditions are expected to be most robust when applying identical methods and conditions at all locations. These conditions were not fulfilled in our study. On one hand, site characteristics vary between the stations, which may influence the sensitivity of PBAP emission to surrounding conditions. On the other hand, the measurements are made with different instruments. The measurement series at Karlsruhe, Germany, are done with a WIBS-4 instrument which includes technical improvements compared to the WIBS-3 used at Manchester, UK and Cork, Ireland (Gabey et al., 2010; Healy et al., 2012b). At Hyytiälä, Finland, and Killarney, Ireland, the UV-APS is used to determine the FBAP concentration. This variation may lead to different estimation of the FBAP concentration and within this case study WIBS may report FBAP at lower concentrations than UV-APS at different locations but similar meteorological conditions.

In this paper, fungal spore concentrations are calculated with the COSMO-ART atmospheric model by using literature-based emission parameterizations which adapt simulated global atmospheric concentration to mannitol measurements or spore colony

ACPD
14, 9903–9950, 2014

counts (Heald and Spracklen, 2009; Sesartic and Dallafior, 2011). The temporal development of the simulated concentrations calculated by COSMO-ART approximately reproduces the measured FBAP concentrations. A diurnal cycle in the simulated fungal spore concentrations with a maximum between midnight and sunrise is probably influenced by boundary layer compression at night. Measured FBAP concentrations are often not consistent to simulated h_{PBL} which suggest that $N_{F,c}$ is additionally influenced by increases in biological emission at night.

The purpose of the work reported here was to develop a new emission parameterization for fungal spores, because literature-based emissions for fungal spores have been found to significantly underestimate measured FBAP concentrations. The parameterization is therefore adjusted to the FBAP concentrations (Sect. 3.2). As was formulated by Heald and Spracklen (2009), it depends on the specific humidity and the leaf area index, but is extended by temperature. The resulting concentrations are in better agreement to the measured FBAP concentrations on the average, but variations in the measurements are not always captured by the simulation. Another long-term analysis of FBAP concentrations and surrounding conditions may result in a further adjustment of the parameters or reveal another parameter driving the emission.

Using the new emission parameterization on a model domain for Europe, fungal spore emission fluxes are extrapolated from northern parts of the domain, where UV-LIF measurements were located, also to Southern Europe. There, much higher emission fluxes occur in the simulation, partially caused by higher specific humidity, which is also the case for $F_{H\&S}$, as well by temperature dependence in F_{FBAP}. This extrapolation is without local Southern European measurements, however, and thus further UV-LIF measurements are recommended for this region in Southern Europe where fungal spore emission fluxes are potentially greater.

As a result of the relatively low horizontal resolution, small-scale variations influencing fungal spore emission at the measurement sites may not be resolved. Influences on a small scale might be due to an increased amount of fungi for the given vegetation type. When taking the leaf area index as a surrogate for the vegetation type,

ACPD
14, 9903–9950, 2014

uncertainties may result from an insufficient relation to the presence of fungi or additional surrounding factors favoring fungi growth. Furthermore, variations in precipitation may not be captured by the model, which then may lead to improper fungal spore concentrations. The same holds for small wind gusts and convective cells which may have a strong influence on spore dispersion, but are not captured well in the model. An increase in fungal spore concentration during or shortly after rain events (Huffman et al., 2013) could not be reproduced by the simulations, as this effect is not included in the emission parameterization to an adequate extent.

The module calculating the dispersion of fungal spores does not include all processes of aerosol dynamics and cloud physics. Of the processes not included, only breaking up of spores can enhance their number concentration. Coagulation is neglected, as in most cases the fungal spore number concentration is low and, hence, their collision is highly improbable. A coagulation of spores with other aerosol particles is more likely to happen, but not included in the simulations. Not much is known about the role of fungal spores in clouds and their ability to act as cloud condensation nuclei.

The simulations presented in this paper highlight the importance of PBAP to the composition of atmospheric aerosol. Fungal spores, the focus of this paper, are among the main contributors to PBAP and therefore exert significant influence on aerosol loading. In this study, COSMO-ART is used up to simulate all major chemical aerosol compounds except for mineral dust in a domain covering Western Europe. When averaging the mass concentration horizontally across the land-covered part of the model domain and over all time steps of the simulation, fungal spores are among the major mass components (Fig. 10). However, the fraction of fungal spores might be overestimated here, as another major aerosol component, mineral dust, is not included, because the domain does not include any desert dust source areas. An additional difference in the treatment of aerosol dynamics implies that spores in the simulation are assumed to be monodisperse with a diameter of 3 µm without being subjected to sedimentation.

A FBAP mass concentration, estimated from measured FBAP number concentrations ($d_p = 3\,\mu m$; $\rho_p = 1\,g\,cm^{-3}$), may reach up to 64 % of simulated near-surface

ACPD
14, 9903–9950, 2014

chemical aerosol mass components in rural areas of Finland (Table 2). In comparison to relations of PBAP to total aerosol concentrations given in literature, their volume fraction of particles larger than 0.2 µm during one year of measurements at a remote site in Siberia reaches 28 % on the average and at Mainz, Germany the volume fraction amounts to 22 % (Matthias-Maser et al., 2000). Both of these fractions agree well with simulated mass fractions of this study for comparable locations, but simulated concentrations given in this study are much lower than total number concentrations given in Matthias-Maser et al. (2000). In contrast, the number and mass fractions in the Amazonian basin are above 80 % and therefore much higher than in the highlighted urban and remote areas (Pöschl et al., 2010), but here the absolute concentrations are less and therefore in the order of magnitude given by the simulation of this study.

PBAP and especially fungal spores might account for a major part of the aerosol loading. Locally, a correlation between increasing FBAP and ice nuclei number concentration (Tobo et al., 2013) shows that future model studies of PBAP impacts on clouds are needed to determine their relevance to atmospheric ice nucleation.

Acknowledgements. We wish to thank A. Schnur for preliminary studies in connection with this paper and M. Bangert for technical support. We would like to thank the EMPA members, particularly C. Knote and D. Brunner, for providing the emission data of the chemical compounds. We also wish to acknowledge P. Aalto, V. Hiltunen, T. Petäjä, C. Schumacher, and M. Kulmala for assistance gathering and analyzing data. We acknowledge support by the Deutsche Forschungsgemeinschaft and the Open Access Publishing Fund of the Karlsruhe Institute of Technology. This research was funded by the Helmholtz Association through the Helmholtz Climate Initiative REKLIM, the President's Initiative and Networking Fund and by DFG through project HO 4612/1-1 (FOR 1525 INUIT). J. A. Huffman acknowledges internal faculty funding from the University of Denver. J. A. Huffman, C. Pöhlker, and U. Pöschl acknowledge financial support from the Max Planck Society (MPG), the Max Planck Graduate Center with the Johannes Gutenberg University Mainz (MPGC), the LEC Geocycles Mainz, and the German Research Foundation (DFG PO1013/5-1, FOR 1525 INUIT).

ACPD
14, 9903–9950, 2014

The service charges for this open access publication have been covered by a Research Centre of the Helmholtz Association.

References

Ariya, P. A., Sun, J., Eltouny, N. A., Hudson, E. D., Hayes, C. T., and Kos, G.: Physical and chemical characterization of bioaerosols – Implications for nucleation processes, Int. Rev. Phys. Chem., 28, 1–32, 2009.

Aylor, D. E.: Settling speed of corn (Zea mays) pollen, J. Aerosol Sci., 33, 1601–1607, doi:10.1016/S0021-8502(02)00105-2, 2002.

Bartholomé, E. and Belward, A. S.: GLC2000: a new approach to global land cover mapping from Earth observation data, Int. J. Remote Sens., 26, 1959–1977, doi:10.1080/01431160412331291297, 2005.

Bauer, H., Schueller, E., Weinke, G., Berger, A., Hitzenberger, R., Marr, I. L., and Puxbaum, H.: Significant contributions of fungal spores to the organic carbon and to the aerosol mass balance of the urban atmospheric aerosol, Atmos. Environ., 42, 5542–5549, doi:10.1016/j.atmosenv.2008.03.019, 2008.

Bones, D. L., Henricksen, D. K., Mang, S. A., Gonsior, M., Bateman, A. P., Nguyen, T. B., Cooper, W. J., and Nizkorodov, S. A.: Appearance of strong absorbers and fluorophores in limonene-O_3 secondary organic aerosol due to NH_4^+-mediated chemical aging over long time scales, J. Geophys. Res.-Atmos., 115, D05203, doi:10.1029/2009jd012864, 2010.

Brosseau, L. M., Vesley, D., Rice, N., Goodell, K., Nellis, M., and Hairston, P.: Differences in detected fluorescence among several bacterial species measured with a direct-reading particle sizer and fluorescence detector, Aerosol Sci. Tech., 32, 545–558, doi:10.1080/027868200303461, 2000.

Burch, M. and Levetin, E.: Effects of meteorological conditions on spore plumes, Int. J. Biometeorol., 46, 107–117, doi:10.1007/s00484-002-0127-1, 2002.

Burrows, S. M., Elbert, W., Lawrence, M. G., and Pöschl, U.: Bacteria in the global atmosphere – Part 1: Review and synthesis of literature data for different ecosystems, Atmos. Chem. Phys., 9, 9263–9280, doi:10.5194/acp-9-9263-2009, 2009.

ACPD
14, 9903–9950, 2014

Caruana, D. J.: Detection and analysis of airborne particles of biological origin: present and future, Analyst, 136, 4641–4652, doi:10.1039/c1an15506g, 2011.
Christner, B. C., Morris, C. E., Foreman, C. M., Cai, R., and Sands, D. C.: Ubiquity of biological ice nucleators in snowfall, Science, 319, 1214, doi:10.1126/science.1149757, 2008.
DeLeon-Rodriguez, N., Lathem, T. L., Rodriguez-R, L. M., Barazesh, J. M., Anderson, B. E., Beyersdorf, A. J., Ziemba, L. D., Bergin, M., Nenes, A., and Konstantinidis, K. T.: Microbiome of the upper troposphere: species composition and prevalence, effects of tropical storms, and atmospheric implications, P. Natl. Acad. Sci. USA, 110, 2575–2580, doi:10.1073/pnas.1212089110, 2013.
DeMott, P. J. and Prenni, A. J.: New Directions: need for defining the numbers and sources of biological aerosols acting as ice nuclei, Atmos. Environ., 44, 1944–1945, 2010.
Després, V. R., Huffman, J. A., Burrows, S. M., Hoose, C., Safatov, A. S., Buryak, G., Fröhlich-Nowoisky, J., Elbert, W., Andreae, M. O., Pöschl, U., and Jaenicke, R.: Primary biological aerosol particles in the atmosphere: a review, Tellus B, 64, 15598, doi:10.3402/tellusb.v64i0.15598, 2012.
Di Filippo, P., Pomata, D., Riccardi, C., Buiarelli, F., and Perrino, C.: Fungal contribution to size-segregated aerosol measured through biomarkers, Atmos. Environ., 64, 132–140, doi:10.1016/j.atmosenv.2012.10.010, 2013.
Doms, G. and Schättler, U.: A Description of the Nonhydrostatic Regional COSMO-Model, Deutscher Wetterdienst, Offenbach, Germany, 2002.
Elbert, W., Taylor, P. E., Andreae, M. O., and Pöschl, U.: Contribution of fungi to primary biogenic aerosols in the atmosphere: wet and dry discharged spores, carbohydrates, and inorganic ions, Atmos. Chem. Phys., 7, 4569–4588, doi:10.5194/acp-7-4569-2007, 2007.
Fang, Z. G., Ouyang, Z. Y., Zheng, H., and Wang, X. K.: Concentration and size distribution of culturable airborne microorganisms in outdoor environments in Beijing, China, Aerosol Sci. Tech., 42, 325–334, doi:10.1080/02786820802068657, 2008.
Foot, V. E., Kaye, P. H., Stanley, W. R., Barrington, S. J., Gallagher, M., and Gabey, A.: Low-cost real-time multiparameter bio-aerosol sensors, Optically Based Biological and Chemical Detection for Defence IV, 7116, 71160I, doi:10.1117/12.800226, 2008.
Forster, P., Ramaswamy, V., Artaxo, P., Berntsen, T., Betts, R., Fahey, D. W., Haywood, J., Lean, J., Lowe, D. C., Myhre, G., Nganga, J., Prinn, R., Raga, G., Schulz, M., and Dorland, R. V.: Changes in atmospheric constituents and in radiative forcing, in: Climate Change 2007: The Physical Science Basis. Contribution of Working Group I to the Fourth Assessment

ACPD
14, 9903–9950, 2014

Report of the Intergovernmental Panel on Climate Change, edited by: Solomon, S., Qin, D., Manning, M., Chen, Z., Marquis, M., Averyt, K. B., Tignor, M., and Miller, H. L., Cambridge University Press, Cambridge, UK, New York, NY, USA, 2007.

Fountoukis, C. and Nenes, A.: ISORROPIA II: a computationally efficient thermodynamic equilibrium model for K^+–Ca^{2+}–Mg^{2+}–NH_4^+–Na^+–SO_4^{2-}–NO_3^-–Cl^-–H_2O aerosols, Atmos. Chem. Phys., 7, 4639–4659, doi:10.5194/acp-7-4639-2007, 2007.

Fröhlich-Nowoisky, J., Burrows, S. M., Xie, Z., Engling, G., Solomon, P. A., Fraser, M. P., Mayol-Bracero, O. L., Artaxo, P., Begerow, D., Conrad, R., Andreae, M. O., Després, V. R., and Pöschl, U.: Biogeography in the air: fungal diversity over land and oceans, Biogeosciences, 9, 1125–1136, doi:10.5194/bg-9-1125-2012, 2012.

Gabey, A. M., Gallagher, M. W., Whitehead, J., Dorsey, J. R., Kaye, P. H., and Stanley, W. R.: Measurements and comparison of primary biological aerosol above and below a tropical forest canopy using a dual channel fluorescence spectrometer, Atmos. Chem. Phys., 10, 4453–4466, doi:10.5194/acp-10-4453-2010, 2010.

Gabey, A. M., Stanley, W. R., Gallagher, M. W., and Kaye, P. H.: The fluorescence properties of aerosol larger than 0.8 µm in urban and tropical rainforest locations, Atmos. Chem. Phys., 11, 5491–5504, doi:10.5194/acp-11-5491-2011, 2011.

Gabey, A. M., Vaitilingom, M., Freney, E., Boulon, J., Sellegri, K., Gallagher, M. W., Crawford, I. P., Robinson, N. H., Stanley, W. R., and Kaye, P. H.: Observations of fluorescent and biological aerosol at a high-altitude site in central France, Atmos. Chem. Phys., 13, 7415–7428, doi:10.5194/acp-13-7415-2013, 2013.

Graham, B., Guyon, P., Maenhaut, W., Taylor, P. E., Ebert, M., Matthias-Maser, S., Mayol-Bracero, O. L., Godoi, R. H. M., Artaxo, P., Meixner, F. X., Moura, M. A. L., Rocha, C. H. E. D. A., Grieken, R. V., Glovsky, M. M., Flagan, R. C., and Andreae, M. O.: Composition and diurnal variability of the natural Amazonian aerosol, J. Geophys. Res.-Atmos., 108, 4765, doi:10.1029/2003jd004049, 2003.

Gregory, P. H.: The microbiology of the atmosphere, in: Plant Science Monographs, edited by: Polunin, N., Leonard Hill, London, 1961.

Haga, D. I., Iannone, R., Wheeler, M. J., Mason, R., Polishchuk, E. A., Fetch, T., van der Kamp, B. J., McKendry, I. G., and Bertram, A. K.: Ice nucleation properties of rust and bunt fungal spores and their transport to high altitudes where they can cause heterogeneous freezing, J. Geophys. Res.-Atmos., 118, 7260–7272, doi:10.1002/jgrd.50556, 2013.

ACPD
14, 9903–9950, 2014

Hairston, P. P., Ho, J., and Quant, F. R.: Design of an instrument for real-time detection of bioaerosols using simultaneous measurement of particle aerodynamic size and intrinsic fluorescence, J. Aerosol Sci., 28, 471–482, 1997.
Hameed, A. A. A. and Khodr, M. I.: Suspended particulates and bioaerosols emitted from an agricultural non-point source, J. Environ. Monitor., 3, 206–209, 2001.
Heald, C. L. and Spracklen, D. V.: Atmospheric budget of primary biological aerosol particles from fungal spores, Geophys. Res. Lett., 36, L09806, doi:10.1029/2009gl037493, 2009.
Healy, D. A., O'Connor, D. J., Burke, A. M., and Sodeau, J. R.: A laboratory assessment of the Waveband Integrated Bioaerosol Sensor (WIBS-4) using individual samples of pollen and fungal spore material, Atmos. Environ., 60, 534–543, doi:10.1016/j.atmosenv.2012.06.052, 2012a.
Healy, D. A., O'Connor, D. J., and Sodeau, J. R.: Measurement of the particle counting efficiency of the "Waveband Integrated Bioaerosol Sensor" model number 4 (WIBS-4), J. Aerosol Sci., 47, 94–99, doi:10.1016/j.jaerosci.2012.01.003, 2012b.
Healy, D. A., Huffman, J. A., O'Connor, D. J., Pöhlker, C., Pöschl, U., and Sodeau, J. R.: Ambient measurements of biological aerosol particles near Killarney, Ireland: a comparison between real-time fluorescence and microscopy techniques, Atmos. Chem. Phys. Discuss., 14, 3875–3915, doi:10.5194/acpd-14-3875-2014, 2014.
Helbig, N., Vogel, B., Vogel, H., and Fiedler, F.: Numerical modelling of pollen dispersion on the regional scale, Aerobiologia, 20, 3–19, doi:10.1023/b:aero.0000022984.51588.30, 2004.
Hoose, C. and Möhler, O.: Heterogeneous ice nucleation on atmospheric aerosols: a review of results from laboratory experiments, Atmos. Chem. Phys., 12, 9817–9854, doi:10.5194/acp-12-9817-2012, 2012.
Hoose, C., Kristjánsson, J. E., and Burrows, S. M.: How important is biological ice nucleation in clouds on a global scale?, Environ. Res. Lett., 5, 024009, doi:10.1088/1748-9326/5/2/024009, 2010a.
Hoose, C., Kristjánsson, J. E., Chen, J.-P., and Hazra, A.: A classical-theory-based parameterization of heterogeneous ice nucleation by mineral dust, soot, and biological particles in a global climate model, J. Atmos. Sci., 67, 2483–2503, doi:10.1175/2010jas3425.1, 2010b.
Huffman, J. A., Treutlein, B., and Pöschl, U.: Fluorescent biological aerosol particle concentrations and size distributions measured with an Ultraviolet Aerodynamic Particle Sizer (UV-APS) in Central Europe, Atmos. Chem. Phys., 10, 3215–3233, doi:10.5194/acp-10-3215-2010, 2010.

ACPD
14, 9903–9950, 2014

Huffman, J. A., Sinha, B., Garland, R. M., Snee-Pollmann, A., Gunthe, S. S., Artaxo, P., Martin, S. T., Andreae, M. O., and Pöschl, U.: Size distributions and temporal variations of biological aerosol particles in the Amazon rainforest characterized by microscopy and real-time UV-APS fluorescence techniques during AMAZE-08, Atmos. Chem. Phys., 12, 11997–12019, doi:10.5194/acp-12-11997-2012, 2012.

Huffman, J. A., Prenni, A. J., DeMott, P. J., Pöhlker, C., Mason, R. H., Robinson, N. H., Fröhlich-Nowoisky, J., Tobo, Y., Després, V. R., Garcia, E., Gochis, D. J., Harris, E., Müller-Germann, I., Ruzene, C., Schmer, B., Sinha, B., Day, D. A., Andreae, M. O., Jimenez, J. L., Gallagher, M., Kreidenweis, S. M., Bertram, A. K., and Pöschl, U.: High concentrations of biological aerosol particles and ice nuclei during and after rain, Atmos. Chem. Phys., 13, 6151–6164, doi:10.5194/acp-13-6151-2013, 2013.

Jacobson, M. Z. and Streets, D. G.: Influence of future anthropogenic emissions on climate, natural emissions, and air quality, J. Geophys. Res.-Atmos., 114, D08118, doi:10.1029/2008jd011476, 2009.

Jaenicke, R.: Über die Dynamik atmosphärischer Aitkenteilchen, in: Berichte der Bunsengesellschaft für physikalische Chemie, 11, Wiley-VCH Verlag GmbH & Co. KGaA, Weinheim, Germany, 1198–1202, 1978.

Jaenicke, R., Matthias-Maser, S., and Gruber, S.: Omnipresence of biological material in the atmosphere, Environ. Chem., 4, 217–220, doi:10.1071/EN07021, 2007.

Jones, A. M. and Harrison, R. M.: The effects of meteorological factors on atmospheric bioaerosol concentrations – a review, Sci. Total Environ., 326, 151–180, doi:10.1016/j.scitotenv.2003.11.021, 2004.

Kaye, P., Stanley, W. R., Hirst, E., Foot, E. V., Baxter, K. L., and Barrington, S. J.: Single particle multichannel bio-aerosol fluorescence sensor, Opt. Express, 13, 3583–3593, doi:10.1364/opex.13.003583, 2005.

Knote, C., Brunner, D., Vogel, H., Allan, J., Asmi, A., Äijälä, M., Carbone, S., van der Gon, H. D., Jimenez, J. L., Kiendler-Scharr, A., Mohr, C., Poulain, L., Prévôt, A. S. H., Swietlicki, E., and Vogel, B.: Towards an online-coupled chemistry-climate model: evaluation of trace gases and aerosols in COSMO-ART, Geosci. Model Dev., 4, 1077–1102, doi:10.5194/gmd-4-1077-2011, 2011.

Kuenen, J., Denier van der Gon, H., Visschedijk, A., van der Brugh, H., and Gijlswijk, R.: MACC European emission inventory for the years 2003–2007, TNO, Utrecht, Netherlands, TNO-060-UT-2011-00588, 49, 2011.

ACPD
14, 9903–9950, 2014

Lee, H. J., Laskin, A., Laskin, J., and Nizkorodov, S. A.: Excitation–emission spectra and fluorescence quantum yields for fresh and aged biogenic secondary organic aerosols, Environ. Sci. Technol., 47, 5763–5770, doi:10.1021/es400644c, 2013.

Lin, W.-H., and Li, C.-S.: Size characteristics of fungus allergens in the subtropical climate, Aerosol Sci. Tech., 25, 93–100, doi:10.1080/02786829608965382, 1996.

Lundgren, K., Vogel, B., Vogel, H., and Kottmeier, C.: Direct radiative effects of sea salt for the Mediterranean region under conditions of low to moderate wind speeds, J. Geophys. Res.-Atmos., 118, 1906–1923, doi:10.1029/2012jd018629, 2013.

Mahowald, N., Jickells, T. D., Baker, A. R., Artaxo, P., Benitez-Nelson, C. R., Bergametti, G., Bond, T. C., Chen, Y., Cohen, D. D., Herut, B., Kubilay, N., Losno, R., Luo, C., Maenhaut, W., McGee, K. A., Okin, G. S., Siefert, R. L., and Tsukuda, S.: Global distribution of atmospheric phosphorus sources, concentrations and deposition rates, and anthropogenic impacts, Global Biogeochem. Cy., 22, GB4026, doi:10.1029/2008gb003240, 2008.

Martin, S. T., Andreae, M. O., Artaxo, P., Baumgardner, D., Chen, Q., Goldstein, A. H., Guenther, A., Heald, C. L., Mayol-Bracero, O. L., McMurry, P. H., Pauliquevis, T., Pöschl, U., Prather, K. A., Roberts, G. C., Saleska, S. R., Silva Dias, M. A., Spracklen, D. V., Swietlicki, E., and Trebs, I.: Sources and properties of Amazonian aerosol particles, Rev. Geophys., 48, RG2002, doi:10.1029/2008rg000280, 2010.

Matthias-Maser, S., Obolkin, V., Khodzer, T., and Jaenicke, R.: Seasonal variation of primary biological aerosol particles in the remote continental region of Lake Baikal/Siberia, Atmos. Environ., 34, 3805–3811, doi:10.1016/s1352-2310(00)00139-4, 2000.

Morris, C. E., Georgakopoulos, D. G., and Sands, D. C.: Ice nucleation active bacteria and their potential role in precipitation, J. Phys. IV, 121, 87–103, 2004.

Morris, C. E., Sands, D. C., Glaux, C., Samsatly, J., Asaad, S., Moukahel, A. R., Gonçalves, F. L. T., and Bigg, E. K.: Urediospores of rust fungi are ice nucleation active at $> -10\,^{\circ}C$ and harbor ice nucleation active bacteria, Atmos. Chem. Phys., 13, 4223–4233, doi:10.5194/acp-13-4223-2013, 2013.

Murray, B. J., O'Sullivan, D., Atkinson, J. D., and Webb, M. E.: Ice nucleation by particles immersed in supercooled cloud droplets, Chem. Soc. Rev., 41, 6519–6554, 2012.

Olson, D. M., Dinerstein, E., Wikramanayake, E. D., Burgess, N. D., Powell, G. V. N., Underwood, E. C., D'Amico, J. A., Itoua, I., Strand, H. E., Morrison, J. C., Loucks, C. J., Allnutt, T. F., Ricketts, T. H., Kura, Y., Lamoreux, J. F., Wettengel, W. W., Hedao, P., and Kassem, K. R.:

ACPD
14, 9903–9950, 2014

Terrestrial ecoregions of the world: a new map of life on Earth, BioScience, 51, 933–938, 2001.
Pan, Y.-l., Holler, S., Chang, R. K., Hill, S. C., Pinnick, R. G., Niles, S., and Bottiger, J. R.: Single-shot fluorescence spectra of individual micrometer-sized bioaerosols illuminated by a 351- or a 266-nm ultraviolet laser, Opt. Lett., 24, 116–118, doi:10.1364/ol.24.000116, 1999.
Penner, J. E.: Carbonaceous aerosols influencing atmospheric radiation: black and organic carbon, in: Aerosol Forcing of Climate, edited by: Charlson, R. J. and Heintzenberg, J., John Wiley and Sons, Chichester, 91–108, 1995.
Petters, M. D. and Kreidenweis, S. M.: A single parameter representation of hygroscopic growth and cloud condensation nucleus activity, Atmos. Chem. Phys., 7, 1961–1971, doi:10.5194/acp-7-1961-2007, 2007.
Pöhlker, C., Huffman, J. A., and Pöschl, U.: Autofluorescence of atmospheric bioaerosols – fluorescent biomolecules and potential interferences, Atmos. Meas. Tech., 5, 37–71, doi:10.5194/amt-5-37-2012, 2012.
Pöhlker, C., Huffman, J. A., Förster, J.-D., and Pöschl, U.: Autofluorescence of atmospheric bioaerosols: spectral fingerprints and taxonomic trends of pollen, Atmos. Meas. Tech., 6, 3369–3392, doi:10.5194/amt-6-3369-2013, 2013.
Pope, F. D.: Pollen grains are efficient cloud condensation nuclei, Environ. Res. Lett., 5, 044015, doi:10.1088/1748-9326/5/4/044015, 2010.
Pöschl, U., Martin, S. T., Sinha, B., Chen, Q., Gunthe, S. S., Huffman, J. A., Borrmann, S., Farmer, D. K., Garland, R. M., Helas, G., Jimenez, J. L., King, S. M., Manzi, A., Mikhailov, E., Pauliquevis, T., Petters, M. D., Prenni, A. J., Roldin, P., Rose, D., Schneider, J., Su, H., Zorn, S. R., Artaxo, P., and Andreae, M. O.: Rainforest aerosols as biogenic nuclei of clouds and precipitation in the Amazon, Science, 329, 1513–1516, doi:10.1126/science.1191056, 2010.
Prenni, A. J., Petters, M. D., Kreidenweis, S. M., Heald, C. L., Martin, S. T., Artaxo, P., Garland, R. M., Wollny, A. G., and Poschl, U.: Relative roles of biogenic emissions and Saharan dust as ice nuclei in the Amazon basin, Nat. Geosci., 2, 402–405, 2009.
Prenni, A. J., Tobo, Y., Garcia, E., DeMott, P. J., Huffman, J. A., McCluskey, C. S., Kreidenweis, S. M., Prenni, J. E., Pöhlker, C., and Pöschl, U.: The impact of rain on ice nuclei populations at a forested site in Colorado, Geophys. Res. Lett., 40, 227–231, doi:10.1029/2012gl053953, 2013.

ACPD
14, 9903–9950, 2014

Ramankutty, N., Evan, A. T., Monfreda, C., and Foley, J. A.: Farming the planet: 1. Geographic distribution of global agricultural lands in the year 2000, Global Biogeochem. Cy., 22, GB1003, doi:10.1029/2007gb002952, 2008.
Reponen, T., Grinshpun, S. A., Conwell, K. L., Wiest, J., and Anderson, M.: Aerodynamic versus physical size of spores: measurement and implication for respiratory deposition, Grana, 40, 119–125, doi:10.1080/00173130152625851, 2001.
Rinke, R.: Parametrisierung des Auswaschens von Aerosolpartikeln durch Niederschlag, Ph.D. thesis, Inst. für Meteorol. und Klimaforsch., Univ. Karlsruhe (TH), Karlsruhe, Germany, 2008.
Robinson, N. H., Allan, J. D., Huffman, J. A., Kaye, P. H., Foot, V. E., and Gallagher, M.: Cluster analysis of WIBS single-particle bioaerosol data, Atmos. Meas. Tech., 6, 337–347, doi:10.5194/amt-6-337-2013, 2013.
Saari, S. E., Putkiranta, M. J., and Keskinen, J.: Fluorescence spectroscopy of atmospherically relevant bacterial and fungal spores and potential interferences, Atmos. Environ., 71, 202–209, doi:10.1016/j.atmosenv.2013.02.023, 2013.
Schell, B., Ackermann, I. J., Hass, H., Binkowski, F. S., and Ebel, A.: Modeling the formation of secondary organic aerosol within a comprehensive air quality model system, J. Geophys. Res.-Atmos., 106, 28275–28293, 2001.
Schumacher, C. J., Pöhlker, C., Aalto, P., Hiltunen, V., Petäjä, T., Kulmala, M., Pöschl, U., and Huffman, J. A.: Seasonal cycles of fluorescent biological aerosol particles in boreal and semi-arid forests of Finland and Colorado, Atmos. Chem. Phys., 13, 11987–12001, doi:10.5194/acp-13-11987-2013, 2013.
Seinfeld, J. H. and Pandis, S. N.: Atmospheric Chemistry and Physics – From Air Pollution to Climate Change, 2nd Edn., John Wiley & Sons, Hoboken, New Jersey, USA, 2006.
Sesartic, A. and Dallafior, T. N.: Global fungal spore emissions, review and synthesis of literature data, Biogeosciences, 8, 1181–1192, doi:10.5194/bg-8-1181-2011, 2011.
Shaffer, B. T. and Lighthart, B.: Survey of culturable airborne bacteria at four diverse locations in Oregon: urban, rural, forest, and coastal, Microb. Ecol., 34, 167–177, doi:10.1007/s002489900046, 1997.
Tobo, Y., Prenni, A. J., DeMott, P. J., Huffman, J. A., McCluskey, C. S., Tian, G., Pöhlker, C., Pöschl, U., and Kreidenweis, S. M.: Biological aerosol particles as a key determinant of ice nuclei populations in a forest ecosystem, J. Geophys. Res.-Atmos., 118, 100–110, doi:10.1002/jgrd.50801, 2013.

ACPD
14, 9903–9950, 2014

Toprak, E. and Schnaiter, M.: Fluorescent biological aerosol particles measured with the Waveband Integrated Bioaerosol Sensor WIBS-4: laboratory tests combined with a one year field study, Atmos. Chem. Phys., 13, 225–243, doi:10.5194/acp-13-225-2013, 2013.

Trail, F., Gaffoor, I., and Vogel, S.: Ejection mechanics and trajectory of the ascospores of Gibberella zeae (anamorph Fuarium graminearum), Fungal Genet. Biol., 42, 528–533, doi:10.1016/j.fgb.2005.03.008, 2005.

Vogel, B., Vogel, H., Bäumer, D., Bangert, M., Lundgren, K., Rinke, R., and Stanelle, T.: The comprehensive model system COSMO-ART – Radiative impact of aerosol on the state of the atmosphere on the regional scale, Atmos. Chem. Phys., 9, 8661–8680, doi:10.5194/acp-9-8661-2009, 2009.

Vogel, H., Pauling, A., and Vogel, B.: Numerical simulation of birch pollen dispersion with an operational weather forecast system, Int. J. Biometeorol., 52, 805–814, doi:10.1007/s00484-008-0174-3, 2008.

Winiwarter, W., Bauer, H., Caseiro, A., and Puxbaum, H.: Quantifying emissions of primary biological aerosol particle mass in Europe, Atmos. Environ., 43, 1403–1409, doi:10.1016/j.atmosenv.2008.01.037, 2009.

Yamamoto, N., Bibby, K., Qian, J., Hospodsky, D., Rismani-Yazdi, H., Nazaroff, W. W., and Peccia, J.: Particle-size distributions and seasonal diversity of allergenic and pathogenic fungi in outdoor air, ISME J., 6, 1801–1811, 2012.

ACPD
14, 9903–9950, 2014

Table 1. Overview of the measurement sites, including their geographical location and the types of instrument used (d_p corresponds to the optical particle diameter and d_a to the aerodynamic particle diameter). The sections below show the simulation periods and the availability of data at this site (filled dot). Mean values for the simulated meteorological and surface conditions used for the new emission parameterization (Sect. 3.2) at the measurement site during the corresponding time periods are added to each section.

location	Karlsruhe, Germany	Hyytiälä, Finland	Manchester, UK	Killarney, Ireland
coordinates	49°5′43.6″ N 8°25′45.0″ E	61°50′41.0″ N 24°17′17.4″ E	53°27′57.0″ N 2°13′56.0″ W	52°3′28.0″ N 9°30′16.4″ W
altitude	111 m a.s.l.	152 m a.s.l.	45 m a.s.l.	34 m a.s.l.
instrument	WIBS-4	UV-APS	WIBS-3	UV-APS
size range	$0.8 \le d_p \le 16\,\mu m$	$1 < d_a \le 20\,\mu m$	$0.8 \le d_p \le 20\,\mu m$	$1 < d_a \le 20\,\mu m$
22 Jul–28 Jul 2010	•	•	∘	∘
LAI ($m^2\,m^{-2}$)	3.18	3.72	–	–
mean T (°C)	17.3	16.2	–	–
mean q_v ($kg\,kg^{-1}$)	0.0088	0.0108	–	–
26 Aug–1 Sep 2010	•	•	•	•
LAI ($m^2\,m^{-2}$)	2.94	3.4	2.87	2.06
mean T (°C)	16.6	8.5	11.6	11.1
mean q_v ($kg\,kg^{-1}$)	0.0099	0.0067	0.0073	0.0072
11 Oct–21 Oct 2010	•	•	∘	∘
LAI ($m^2\,m^{-2}$)	1.49	1.27	–	–
mean T (°C)	6.5	−0.6	–	–
mean q_v ($kg\,kg^{-1}$)	0.0055	0.0034	–	–

ACPD
14, 9903–9950, 2014

Table 2. Simulated aerosol mass concentrations for aerosol chemical components, including fungal spores, together with measured FBAP values in $\mu g\,m^{-3}$ at the measuring sites as averages over the time period during August 2010.

Particle Mass ($\mu g\,m^{-3}$)	Karlsruhe, Germany	Hyytiälä, Finland	Manchester, UK	Killarney, Ireland
measured FBAP	0.46	0.81	0.19	0.19
simulated fungal spores	0.41	0.20	0.35	0.28
sea salt	0.44	0.01	1.62	1.11
soot	0.19	0.06	0.42	0.04
SO_4^{2-}	0.18	0.01	0.11	0.05
NH_4^+	0.44	0.1	0.14	0.07
NO_3^-	1.29	0.01	0.34	0.18
SOA	0.41	0.24	0.14	0.04
aPOA	0.67	0.13	0.85	0.11

ACPD
14, 9903–9950, 2014

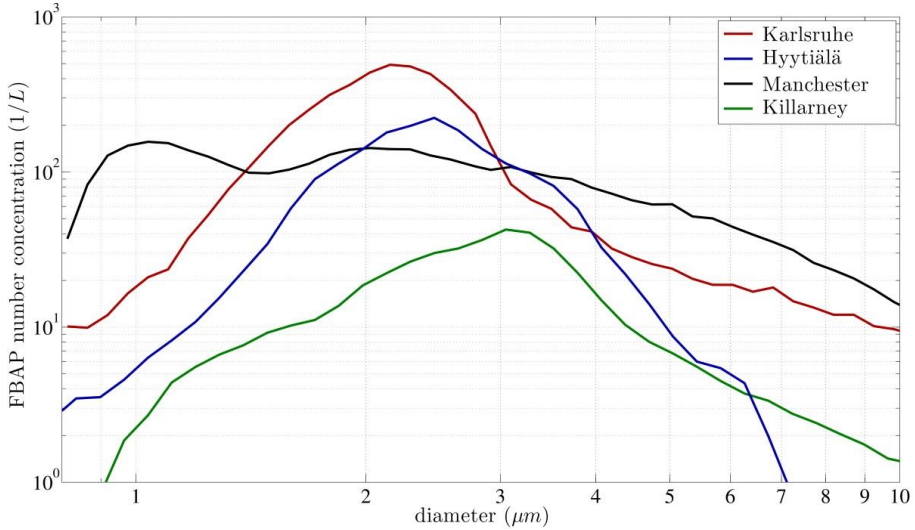

Fig. 1. Average FBAP size distributions derived from UV-LIF measurements during case studies in August 2010 at Karlsruhe (Germany), Hyytiälä (Finland), Manchester (UK), and Killarney (Ireland).

ACPD
14, 9903–9950, 2014

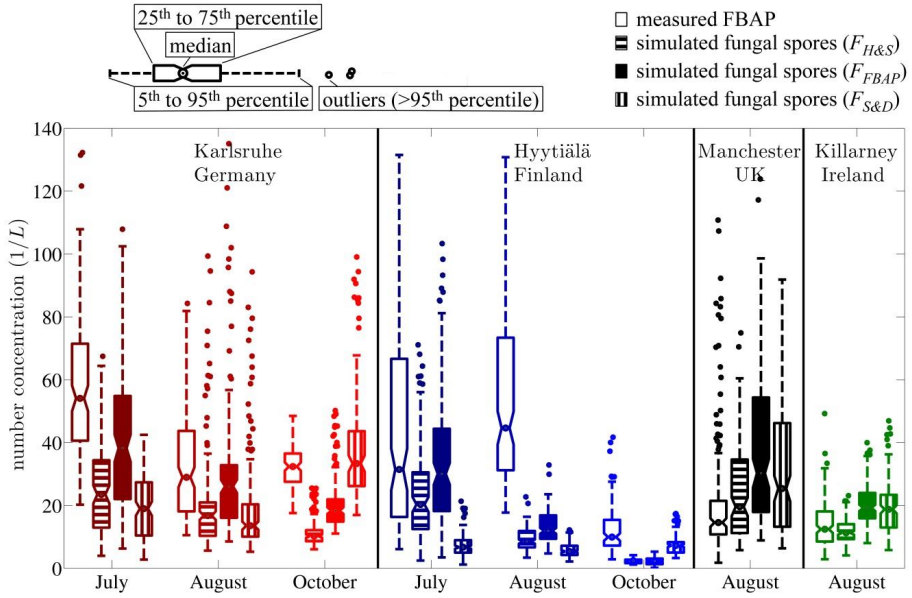

Fig. 2. Box-whisker plots of: measured hourly FBAP concentration (open boxes), simulated fungal spore concentration emitted by $F_{H\&S}$ (horizontally hatched boxes), F_{FBAP} (filled boxes), and $F_{S\&D}$ (vertically hatched boxes) for all case studies. The central mark of each box shows the median, its edges the 25th and 75th percentiles, and whiskers show 5th and 95th percentiles. Dotes above whisker show outliers (> 95th percentile).

ACPD
14, 9903–9950, 2014

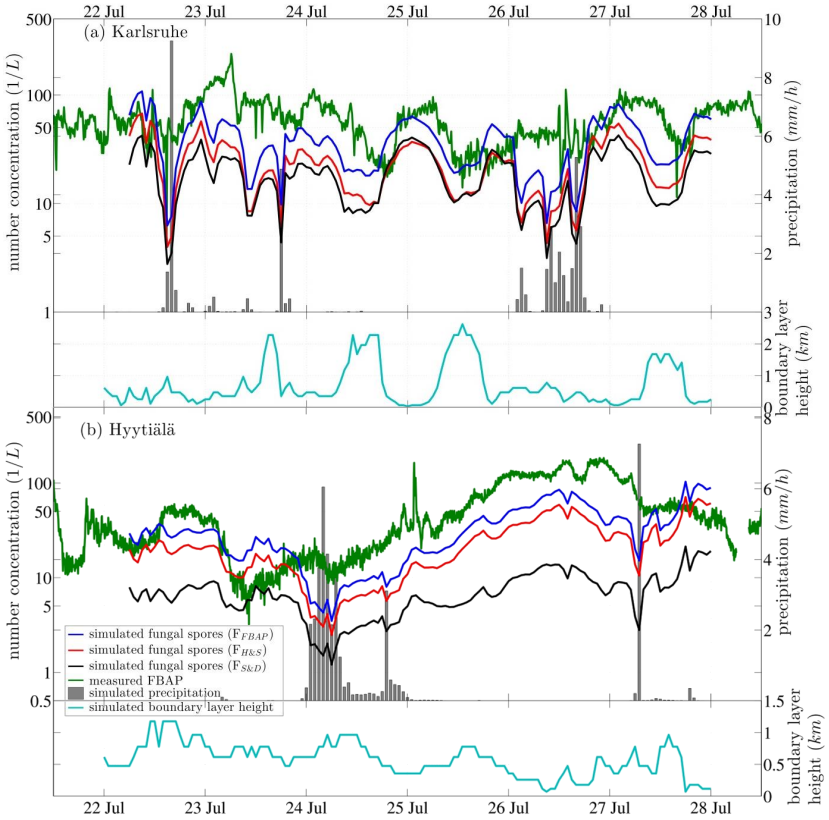

Fig. 3. Time series of measured FBAP and simulated fungal spore number concentrations in L^{-1} together with simulated precipitation in $mm\,h^{-1}$ (right axis) and simulated boundary layer height in km (right axis) during the case study from 22 July to 28 July 2010 at **(a)** Karlsruhe, Germany and **(b)** Hyytiälä, Finland. Simulations were performed with three different emission parameterizations: $F_{H\&S}$ from Heald and Spracklen (2009); $F_{S\&D}$ from Sesartic and Dallafior (2011); F_{FBAP} from this study.

ACPD
14, 9903–9950, 2014

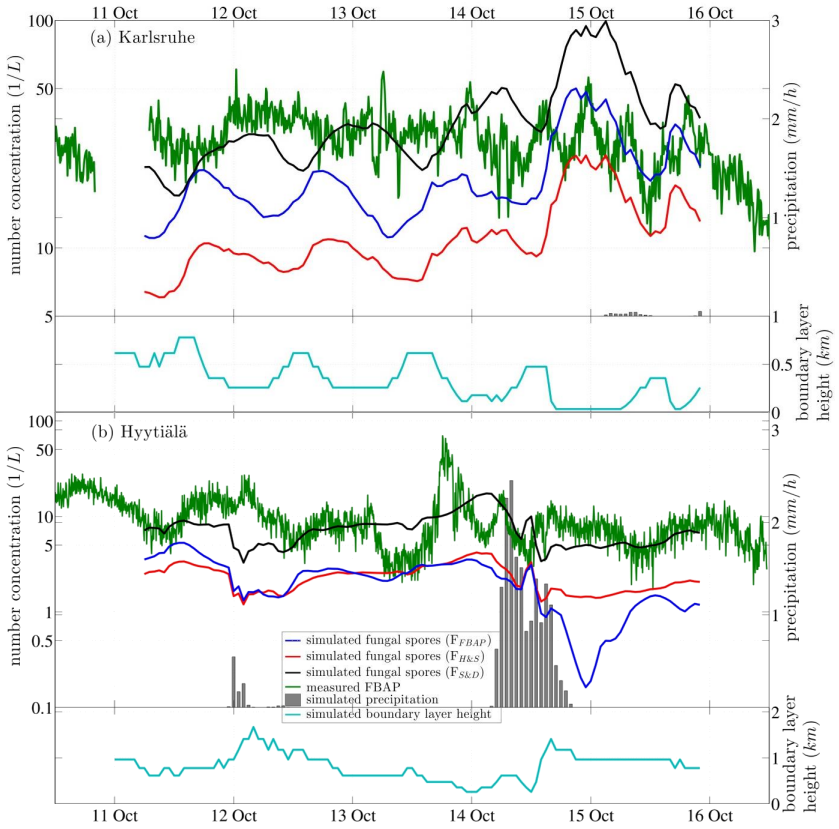

Fig. 4. Time series of measured FBAP and simulated fungal spore number concentrations in L^{-1} together with simulated precipitation in $mm\,h^{-1}$ (right axis) and simulated boundary layer height in km (right axis) during the case study from 11 October to 21 October 2010 at **(a)** Karlsruhe, Germany and **(b)** Hyytiälä, Finland. Simulations were performed with three different emission parameterizations: $F_{H\&S}$ from Heald and Spracklen (2009); $F_{S\&D}$ from Sesartic and Dallafior (2011); F_{FBAP} from this study.

ACPD
14, 9903–9950, 2014

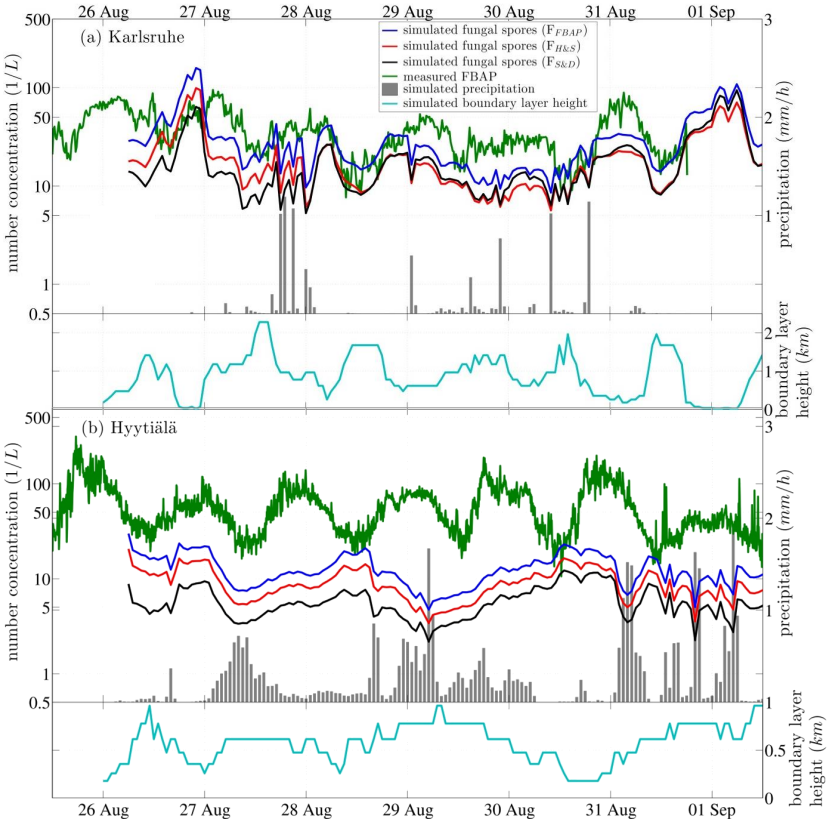

Fig. 5. Time series of measured FBAP and simulated fungal spore number concentrations in L^{-1} together with simulated precipitation in $mm\,h^{-1}$ (right axis) and simulated boundary layer height in km (right axis) during the case study from 26 August to 1 September 2010 at **(a)** Karlsruhe, Germany. **(b)** Hyytiälä, Finland. Simulations were performed with three different emission parameterizations: $F_{H\&S}$ from Heald and Spracklen (2009); $F_{S\&D}$ from Sesartic and Dallafior (2011); F_{FBAP} from this study.

ACPD
14, 9903–9950, 2014

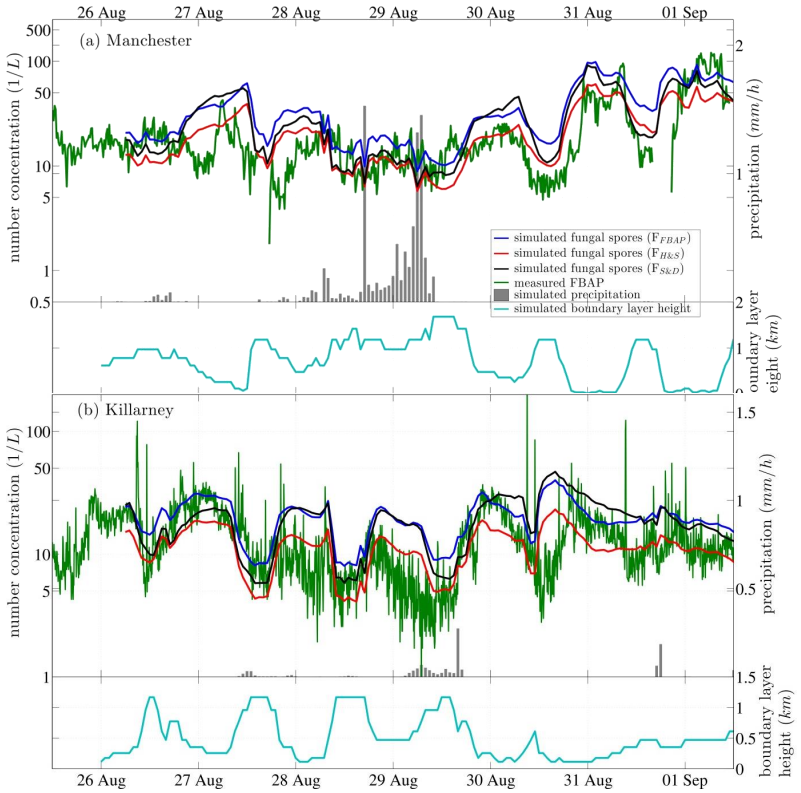

Fig. 6. Time series of measured FBAP and simulated fungal spore number concentrations in L^{-1} together with simulated precipitation in $mm\,h^{-1}$ (right axis) and simulated boundary layer height in km (right axis) during the case study from 26 August to 1 September 2010 at **(a)** Manchester, UK and **(b)** Killarney, Ireland. Simulations were performed with three different emission parameterizations: $F_{H\&S}$ from Heald and Spracklen (2009); $F_{S\&D}$ from Sesartic and Dallafior (2011); F_{FBAP} from this study.

ACPD
14, 9903–9950, 2014

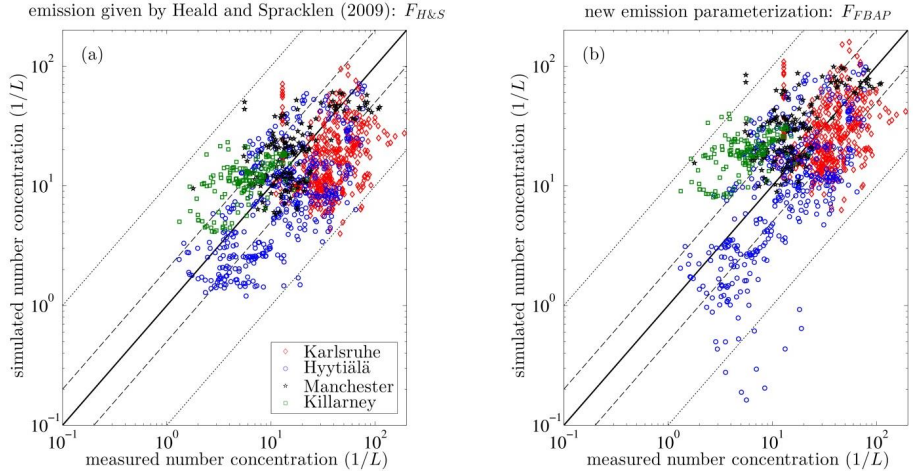

Fig. 7. Comparison for all case studies: measured FBAP number concentrations plotted vs. simulated fungal spore number concentrations **(a)** based on Heald and Spracklen (2009) emission flux and **(b)** based on emission parameterization derived from a multiple linear regression to FBAP concentrations. Solid black lines represent the 1 : 1-line, dashed lines the 1 : 2-line and dotted lines the 1 : 10-line.

ACPD
14, 9903–9950, 2014

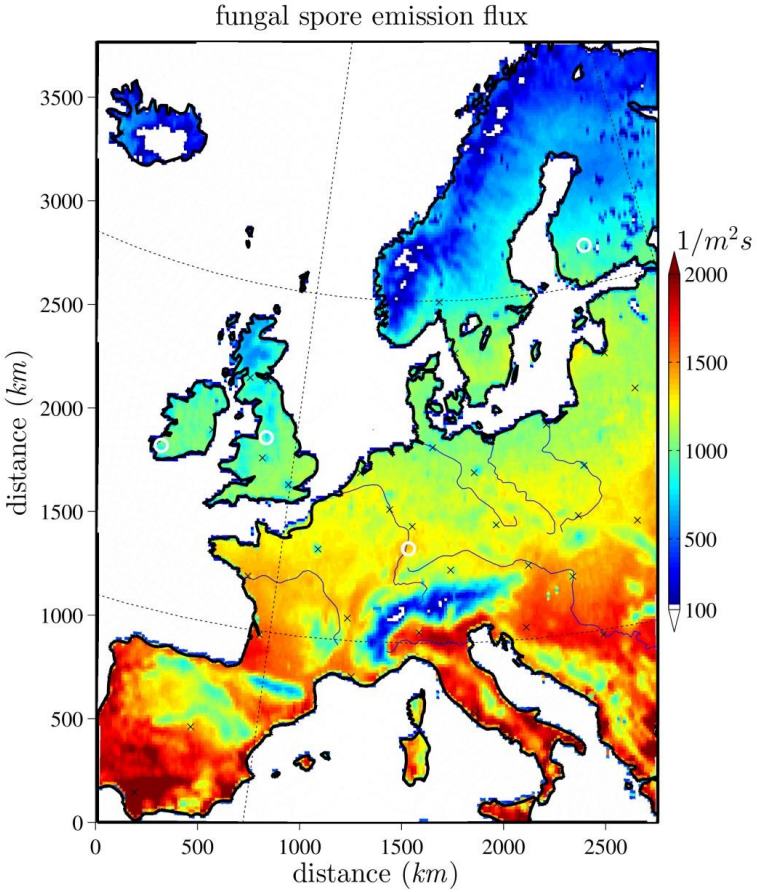

Fig. 8. Average simulated fungal spore emission flux (F_{FBAP}) in $\mathrm{m}^{-2}\,\mathrm{s}^{-1}$ from 26 August to 1 September 2010, (excluding a spin-up period of 6 h). White circles indicate the locations of the different FBAP measurement time series.

ACPD
14, 9903–9950, 2014

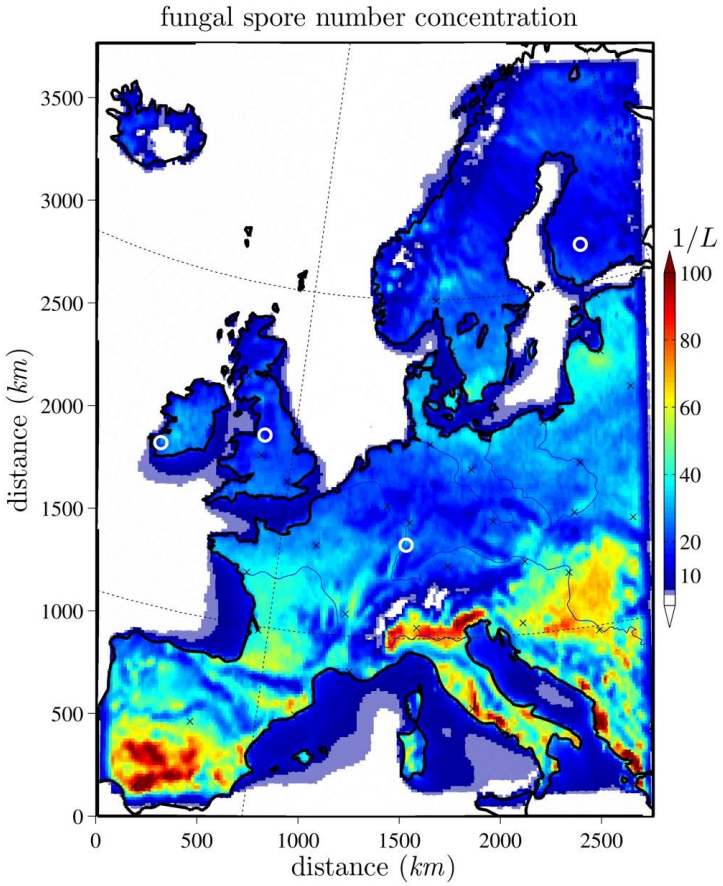

Fig. 9. Horizontally distributed fungal spore concentration in L^{-1}, emitted by F_{FBAP}, in the lowest model layer, averaged from 26 August to 1 September 2010 (excluding a spin-up period of 6 h). White circles indicate the locations of the different FBAP measurement time series.

ACPD
14, 9903–9950, 2014

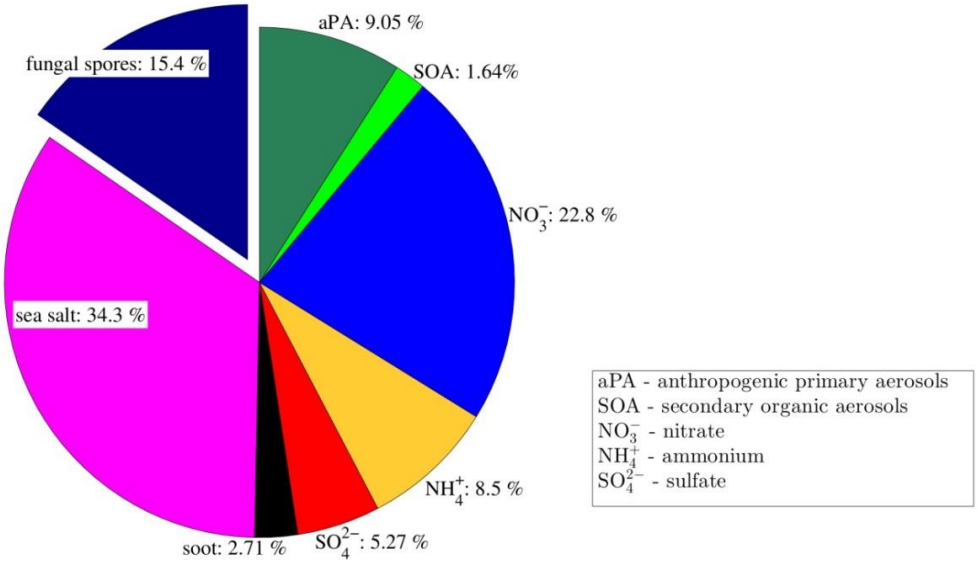

Fig. 10. Near-surface chemical aerosol mass composition simulated by COSMO-ART, horizontally averaged over the land area in the model domain and temporally averaged from 26 August to 1 September 2010 (excluding a spin-up period of 6 h).

ACPD
14, 9903–9950, 2014